ENHANCED UAV NAVIGATION USING HALL-MAGNETIC AND AIR-MASS FLOW SENSORS IN INDOOR ENVIRONMENT

S.Zahran [1], A.Moussa [1,2], N. El-Sheimy [1]

[1] Dept. of Geomatics Engineering, University of Calgary, Calgary, AB, Canada – (Shady.zahran1, elsheimy)@ucalgary.ca
[2] Department of Electrical Engineering, Port-Said University, Port Said, Egypt – amelsaye@ucalgary.ca

Commission I, ICWG I/II

KEY WORDS: Hall-Effect Sensor, Mass-Flow Sensor, Extended Kalman Filter, Odometer, Sensors Fusion.

ABSTRACT:

The use of Unmanned Aerial Vehicles (UAVs) in many commercial and emergency applications has the potential to dramatically alter several industries, and, in the process, change our attitudes regarding their impact on our daily lives activities. The navigation system of these UAVs mainly depends on the integration between the Global Navigation Satellite Systems (GNSS) and Inertial Navigation System (INS) to estimate the positions, velocities, and attitudes (PVT) of the UAVs. However, GNSS signals are not always available everywhere and therefore during GNSS signal outages, the navigation system performance will deteriorate rapidly especially when using low-cost INS. Additional aiding sensors are required, during GNSS signal outages, to bound the INS errors and enhance the navigation system performance. This paper proposes the utilization of two sensors (Hall-magnetic and Air-Mass flow sensors) to act as flying odometer by estimating the UAV forward velocity. The estimated velocity is then integrated with INS through Extended Kalman Filter (EKF) to enhance the navigation solution estimation. A real experiment was carried out with the 3DR quadcopter while the proposed system is attached on the top of the quadcopter. The results showed great enhancement in the navigation system performance with more than 98% improvement when compared to the free running INS solution (dead-reckoning).

1. INTRODUCTION

UAVs applications have spread widely during the past decade, due to their mobility, that makes these UAVs able to accomplish different applications (Valavanis and Vachtsevanos, 2015) while saving cost, time, effort and not exposing human lives to danger. For UAVs to be capable of performing different tasks in all environments, the navigation system must be versatile and able to estimate the navigation parameters with acceptable performance according to its required tasks. The navigation system mainly depends on the integration between the output of the INS mechanization process, and the GNSS system (Noureldin et al., 2013). Typically, low-cost/commercial small UAVs utilize low-cost Micro Electro Mechanical Systems (MEMS) based INS to estimate the UAVs navigation parameters. However, MEMS-based INS. When working in stand-alone, suffer from a massive accumulation of errors that will deteriorate the navigation solution ("Enhanced UAV navigation in GNSS denied environment using repeated dynamics pattern recognition - IEEE Conference Publication," n.d.). In typical scenarios, GNSS is integrated with INS to bound its errors. The problem arises once the GNSS signals are lost, which will affect the ability of the UAV to navigate for longer periods. To assure the ability of the UAV to accomplish its tasks even during GNSS signals unavailability, other sensors must be employed to replace the GNSS role and bound the INS drift and enhance the navigation performance.

Many solutions had been investigated to compensate the GNSS signals outage periods. One of the potential solutions is based on vision aiding (Mostafa et al., n.d.) (Zhang et al., 2014) (Wang et al., 2013) or vision-based (Lu et al., 2018; Sheta, 2012) navigation systems. In case of vision-aided navigation, the measurements of single/multiple cameras are fused with INS to bound the drift and enhance the navigational solution. Examples of vision-aided navigation include optical flow based approach (OF), which utilize consecutive images to detect and track common features, to estimate the UAV velocity (Mostafa et al., n.d.) (Chao et al., 2013). Another vision aided approach to localize the vehicle based on mosaicking was proposed in (Caballero et al., 2009) . While vision-based navigation mainly relies on matching pre-surveyed features (known coordinates) with images taken by the onboard vision system, to estimate the position of the UAV (Sheta, 2012). While in (Zhang et al., 2011) the position estimation problem is based on particle filter based approach compared to Digital Elevation Map (DEM) for the area of operation. Cameras are consider a good candidate to replace the GNSS system during signal outage periods. However, vision systems are not immune against environmental changes (light condition, rain, etc.), lack of features which will deteriorate the performance, or scale ambiguity which can be solved by using stereo cameras (Mustafah et al., 2012) or other aiding sensors.

Another strong candidate to bound the drift of INS is Laser Imaging Detection and Ranging (LIDAR) (Hemann et al., 2016; Kumar et al., 2017; Tang et al., 2015). One of the most common techniques utilizing such sensor is Simultaneous Localization and Mapping (SLAM). SLAM is constructing a map for the surrounding environment in the same time the UAV is localized (Bailey and Durrant-Whyte, 2006; Mohamed et al., 2017). One of the challenges facing the utilization of LIDAR is the time consumption. Different approaches have been utilized to decrease the computation time as in (Zahran et al., 2018a), they benefited from the Vehicle Dynamic Model (VDM) for that purpose. VDM act as an initialization step, to estimate the vehicle rotation for the scan matching algorithm, without the requirement for any feature for this initialization step. In (Mohamed et al., 2017) they used also initialization step before scan matching. This initialization step based on locating at least one corner feature to decrease the computation time. Another draw-back from utilizing LIDAR is its weight and power consumption which is not suitable with small/micro UAVs.

Because the size, space, weight, cost, and power available on such small/micro UAVs is critical, so other unconventional methods were utilized to aid the navigation estimation. In (Barton, 2012), thermopiles were used to find the difference in temperature between the ground and the sky so they can estimate the attitude of the UAV. While in (Zahran et al., 2018b) they introduced unconventional manipulation from the typical use of Hall-effect magnetic sensor. The proposed approach act as a flying odometer for quadcopter (Air-Odo) to estimate its forward velocity. Air-Odo measurements are integrated with INS through Extended Kalman Filter (EKF) to enhance the navigation solution. Two versions of Air-Odo were shown. First version for low-velocity profiles, and one for higher velocity profiles. Second version was achieved by increasing the weight of the resisting plate. The main drawback of Air-Odo after increasing the resisting plate weight, that it starts measuring the velocities from 2.5m/s.

This paper proposes unconventional approach to enhance the navigation solution, while still preserving the main limitation imposed over these kind of small UAVs (limited size, space, weight, power, and computation). The proposed approach is based on manipulating the typical use of two sensors. Hall-Effect sensor which is typically used to replace potentiometers, robotics joints, angle sensors and ground vehicle RPMs calculations. Second sensor is Air-Mass flow sensor which is typically used in ventilation, inhalers, medical instrument and burner control. Both sensors complement the drawbacks of each other, such that the overall system will be suitable to act as an odometer system for both low and high-velocity profile quadcopter UAV.

2. SYSTEM OVERVIEW

The main objective of the proposed system is to limit the INS drift in the indoor environments or during the GNSS signal unavailability. The proposed approach is based on a merge between two sensors; Hall-effect sensor and air-mass flow sensor. Both sensor where utilized in a completely different way compared to their typical use. The proposed system will act as flying odometer for quadcopter UAV and estimate its velocity. The estimated velocity will be integrated with INS measurements through EKF to estimate better navigation parameters. It is worth noting that the conventional pitot tube used in the fixed wing drones cannot be employed for that type of drones (quadcopters) for these reasons (Zahran et al., 2018b): 1) pitot tube is sensitive to the direction of air flow; 2) it requires high air flow velocity; and 3) small change in velocities of quadcopter did not induce significant differential pressure to be measured by pitot tube.

2.1 Hall-effect Sensor "Higher velocity profile Air-Odo"

Air-Odo is a flying odometer for a quadcopter based on contactless angle rotary magnetic encoder (Hall-effect sensor). Air-Odo is based on the law of immersed bodies in fluid (air). Air-Odo is composed of a static part, two opposite rotating magnets, and a resisting plate as shown in Figure 1. The resisting plate will be rotating from its position because of the airflow caused from quadcopter motion, as shown in Figure 2. This angle represents the speed of the quadcopter according to equations (1-6).

$$L = \frac{1}{2}\rho V^2 A C_D \qquad (1)$$

$$L\,.\cos(\theta) = mg\,.\sin(\theta) \qquad (2)$$

Where: L is the force resulting from the relative airflow (lifting).
ρ is the air density.
V is the velocity of flow.
A is the area of the resisting plate.
C_D is the drag coefficient.
m is the mass of the resisting plate.
g is the gravity constant.
θ is the angle of the resisting plate.

Substituting (1) in (2).

$$\frac{1}{2}\rho V^2 A C_D\,.\cos(\theta) = mg\,.\sin(\theta) \qquad (3)$$

$$\tan(\theta) = \frac{\rho V^2 A C_D}{2mg} \qquad (4)$$

Some of the variables in (4) can be considered as constants for a specific design ($\rho, A, C_D, m, and\ g$). This will lead to (5) and (6).

$$\tan(\theta) = Const\,.\ V^2 \qquad (5)$$

$$const = \frac{\rho A C_D}{2mg} \qquad (6)$$

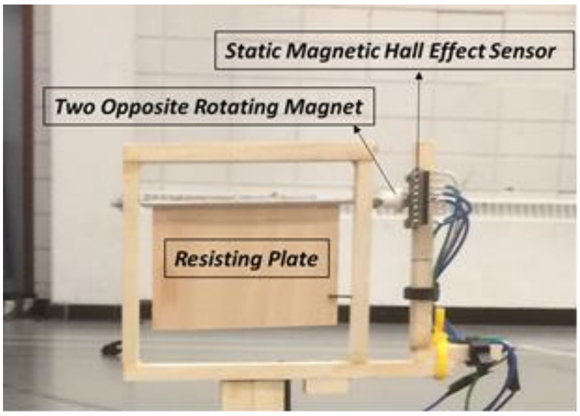

Figure 1. Air-Odo design using Hall-Effect sensor (static and rotating part) and resisting plate.

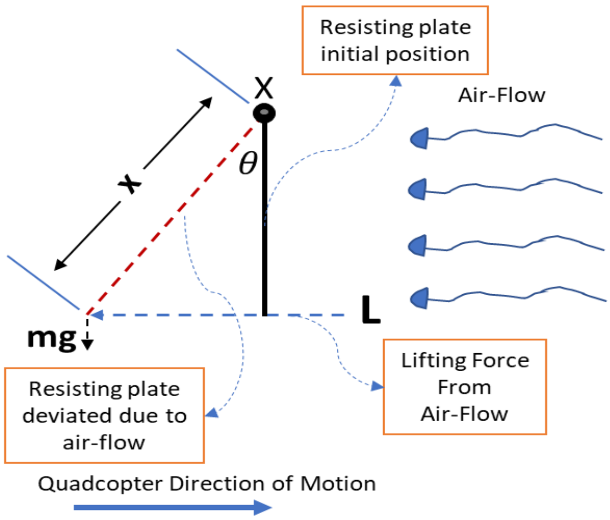

Figure 2. Air-Odo theory of operation-based on law of immersed bodies in fluid (lifting force).

According to the weight of the resisting plate, the dynamic range of velocities that can be measured by Air-Odo can be altered, and the constant value can be calibrated as shown in (Zahran et al., 2018b). In its current state Air-Odo can measure from 0.7 m/s to 5 m/s. By increasing the resisting plate weight (8 grams) as shown in Figure 3, the velocities range changed to be from 2.5m/s up to 10m/s. Figure 4 represents the measurements from Air-Odo with and without weight in a wind tunnel experiment to estimate the constant value shown in equation (6).

Figure 3. Air-Odo with additional weight (8 grams) added to the resisting plate to increase its velocity dynamic range.

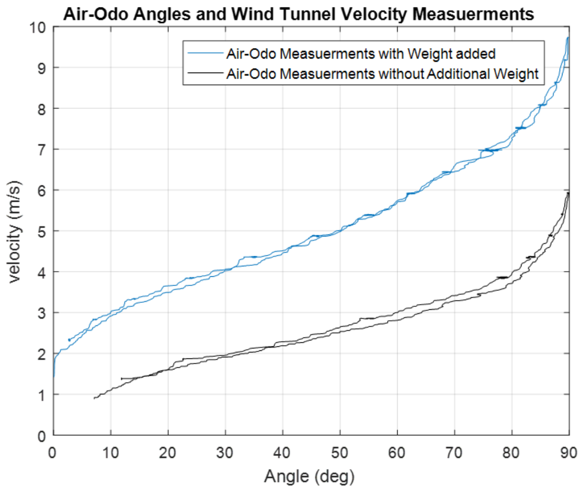

Figure 4. Air-Odo angle measurements and Wind-tunnel velocities relationship.

In order to use the higher velocity dynamic range Air-Odo, another sensor is used to account for the low-velocity profiles "Air-mass flow sensor".

2.2 Air-mass flow sensor

Air-mass flow/ Mass-Flow sensor is shown in Figure 5, the flow meter is typically used in vast applications like medical purposes (respiration applications), Heating, Ventilation, and Air Conditioning (HVAC) applications, burner control, and fuel cell control. In this proposed system Air-mass flow is used as an odometer for quadcopter to measure the induced air resulting from quadcopter motion.

Figure 5. Mass-Flow Sensor

Mass flow meter sensor can measure the flow of air and non-aggressive gases with high output rate up to 2kHz.Although Mass-flow meter can measure higher speeds than the quadcopter velocities, although it is sensitive to the direction of air flow. This sensitivity will limit its capabilities when it is mounted on the quadcopter, because of the way the quadcopter moves. The quadcopter tends to tilt towards the direction of motion, and this tilting angle increase when the velocity increases, which makes the Mass flow meter at higher velocities on board of the quadcopter useless as shown in Figure 6.

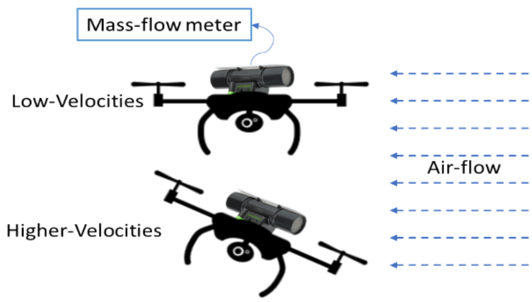

Figure 6. Quadcopter tilting (Higher velocities) and its effect on Mass-Flow meter.

2.3 Fusion Filter

The measurements from both systems (velocity) were fused together based on velocity criteria. The velocity from the Mass-flow meter is considered as long as the velocity is lower than 2.5m/s, and higher than that the velocity is taken from Air-Odo. The overall velocities (output of both system fused together) are integrated with INS measurements through a loosely coupled EKF as shown in Figure 7.

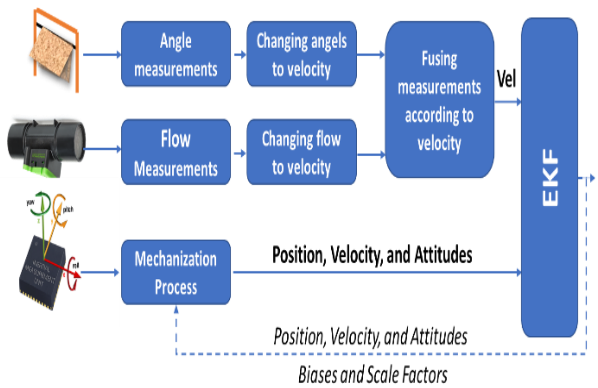

Figure 7. Proposed approach work scheme/integration through Extended Kalman Filter.

3. HARDWARE ASSEMBLY AND EXPERIMENT

3.1 Hardware

The quadcopter used is a commercial small size on the shelf quadcopter (3DR SOLO).This drone is equipped with MEMS-based low-cost IMU (MPU 9000 series), and a U-blox GPS. On the other hand, Air-Odo system and the Mass flow-meter is connected to LattePanda onboard Mini PC for data logging and processing. A flight was conducted indoor to verify the ability of the proposed system to enhance the navigation system parameters estimation during GNSS signal outage. MarvelMind indoor positioning system (consist of 4 stationary beacons distributed around the four corners of the field, and one moving beacon mounted on the quadcopter) was used as a reference solution. The overall system is shown in Figure 8.

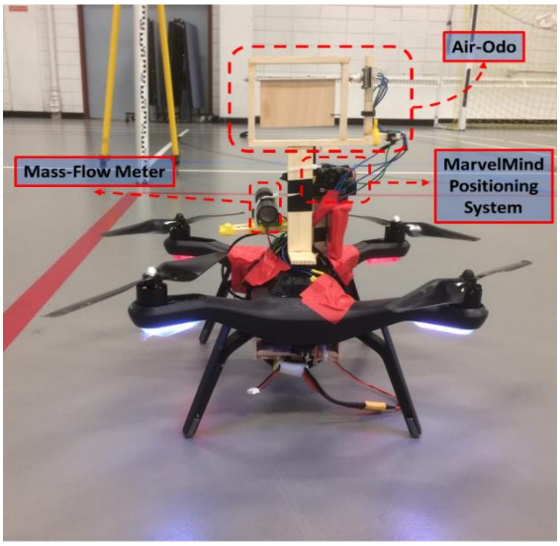

Figure 8. 3DR quadcopter equipped with all the equipment (Air-Odo, Mass-Air flow, and MarvelMind indoor positioning system) for the indoor flying experiment

3.2 Experiment

The flight extended for around 260 seconds, with varying velocities from 0 to 6 m/s. Figure 9 shows the velocity from Air-Odo alone with additional weight added to the resisting plate compared to the reference velocity.

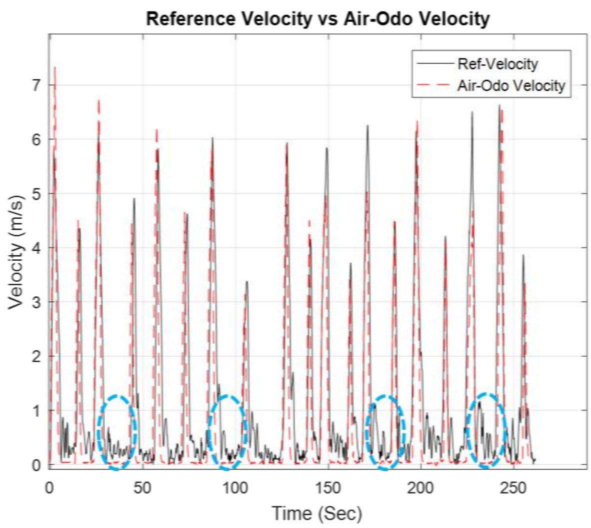

Figure 9. Air-Odo velocity estimation compared to the reference velocity, and the red circles showing that this version of Air-Odo with additional weight can't sense the lower velocities profile.

As shown in the previous figure that Air-Odo can’t sense lower velocities (as shown in the blue circles). Both velocities from Air-Odo and Mass-flow meter will be merged together to account for lower and higher.

Figure 10 shows the benefit of the proposed system (merging the measurements from Air-Odo with additional weight and mass flow sensor) to account for both lower and higher quadcopter velocities.

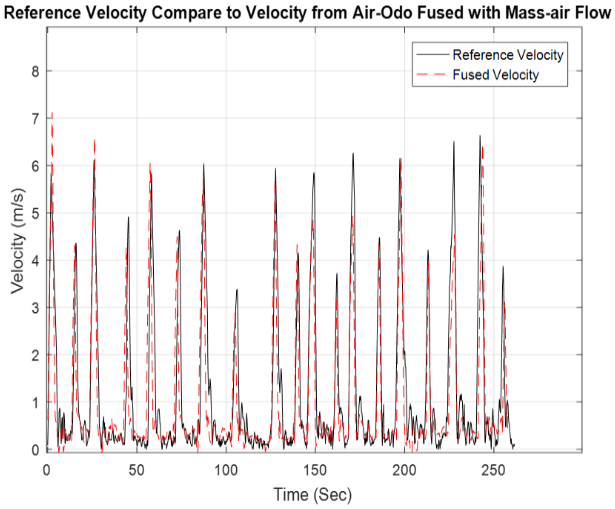

Figure 10. Velocity estimation from the proposed approach (Air-Odo and Mass-Flow sensor) compared to the reference velocity, showing the ability of the proposed system to sense lower and higher velocities compared to Air-Odo alone with additional weight added.

3.2.1 INS Dead-Reckoning Solution: Figure 11 shows the reference trajectory compared to the solution from the INS solution This experiment ensures the inability of the low-cost INS to estimate the navigation unknowns, during the absence of an absolute positioning system.

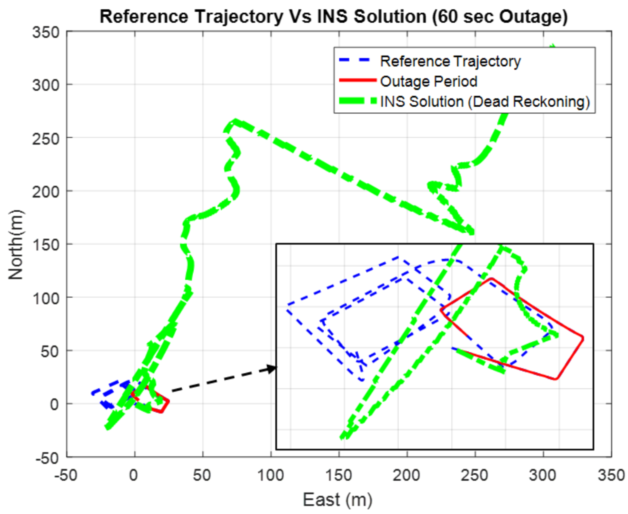

Figure 11. The solution of the INS -Stand alone system during GNSS signal outage is compared to the reference trajectory showing the massive drift happened during this outage period.

Also, Figure 12 and Table 1 show the errors in the north and east direction during this GNSS outage period. The results prove the massive drift happened during this period which reached hundreds of meters.

	INS-Dead-Reckoning Error (m)
RMSE North	140.91
Maximum Error North	332.7
RMSE East	127.14
Maximum Error East	304

Table 1. INS dead-reckoning solution errors during 60 Secs of GNSS signal outage.

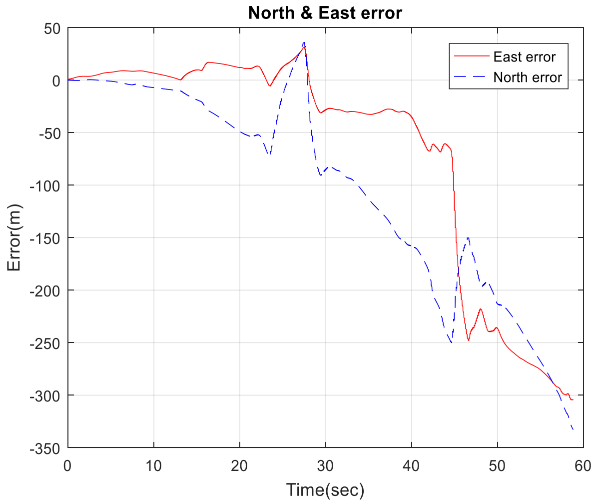

Figure 12. Errors in north and east directions of the INS - Standalone system during GNSS signal outage for 60 Secs.

3.2.2 Air-Odo – INS integration (60 Secs Outage): This test aims to evaluate the performance of the Air-Odo system only with the added additional weight. Figure 13 shows the obtained solution from Air-Odo alone with the additional weight compared to the reference trajectory.

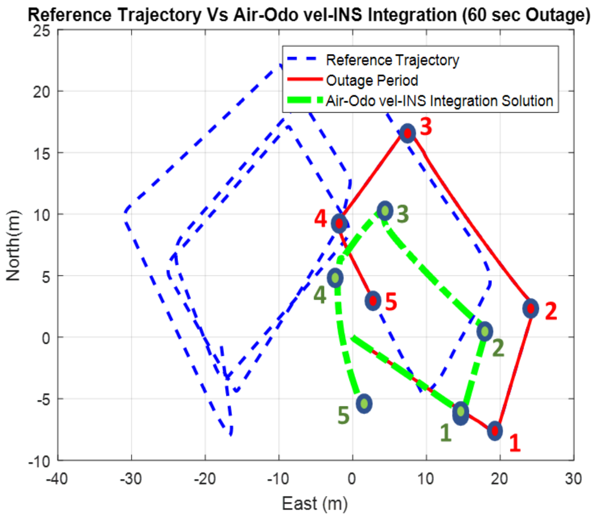

Figure 13. Solution of integrating Air-Odo alone with additional weight and INS during 60 Secs of GNSS signal outage.

As seen in the previous figure that the solution of that integration cause trajectory shrinking, as the Air-Odo system with additional weight can measure velocity starting from 2.5 m/s, and below this velocity it will predict that the quadcopter is hovering (zero velocity).

Table 2 shows the RMSE and maximum errors in both north and east direction. While Figure 14 shows the error trend during the flight in both directions as well.

	Proposed approach - INS Error (m)
RMSE North	4.69
Maximum Error North	13.17
RMSE East	4.37
Maximum Error East	10.08

Table 2. Air-Odo – INS performance during 60 Secs of GNSS signal outage.

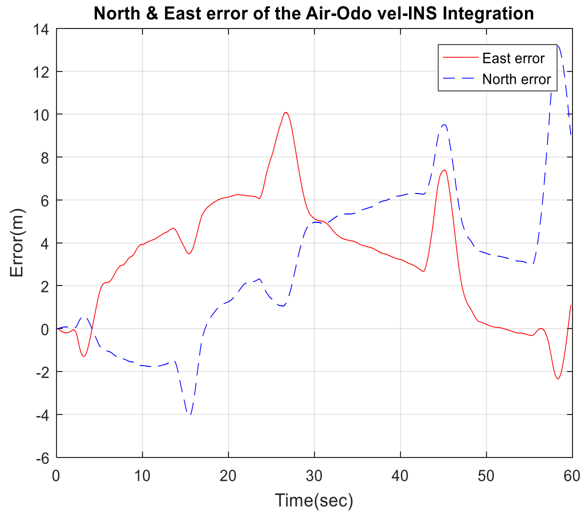

Figure 14. Errors in north and east directions of the Air-Odo alone with additional weight and INS solution during GNSS signal outage for 60 Secs.

3.2.3 Proposed approach- INS integration (60 Secs Outage): The following Figures 15 and 16 show the ability of the proposed approach to limit the drift of the INS during the absence of an absolute positioning system.

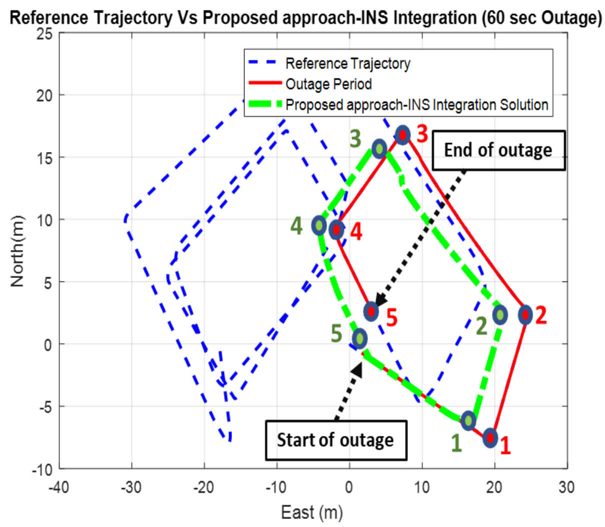

Figure 15. Solution of the proposed approach integrated with INS during 60 Secs of GNSS signal outage.

Both Figures 15 and 16 proved that the proposed approach was able to limit the massive drift exhibited by the INS system as a standalone system. The RMSE reached 2.83 and 1.31 meters in the east and north direction respectively as seen in Table 3.

	Proposed approach - INS Error (m)
RMSE North	1.31
Maximum Error North	4.67
RMSE East	2.83
Maximum Error East	6.39

Table 3. Proposed approach performance errors during 60 Secs of GNSS signal outage.

Comparing Table 3 to Table 2 results, prove the significance of merging between Air-Odo and mass flow sensor to account for lower and higher velocity profiles.

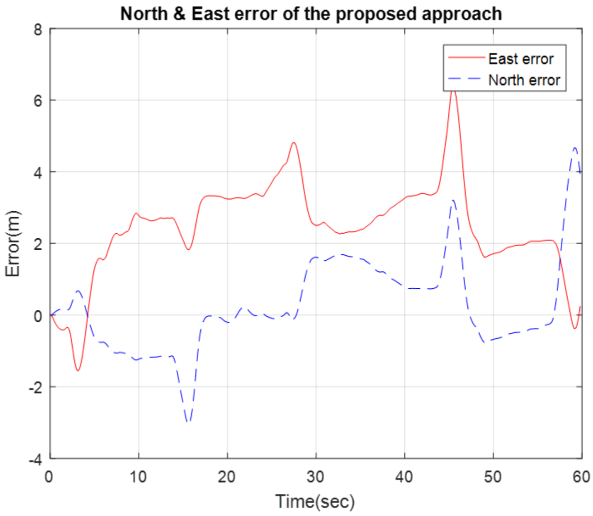

Figure 16. Errors in the north and east direction of the proposed approach integrated with INS during 60 Secs of GNSS signal outage.

3.2.4 Proposed approach- INS integration (120 Secs Outage): This experiment is to show that the proposed approach can limit the drift for a longer outage period (2 min). The integration results between the proposed approach and the reference trajectory are shown in Figure 16.

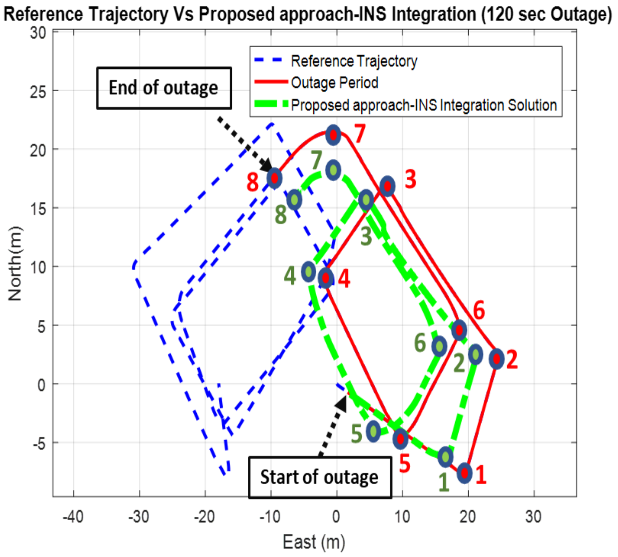

Figure 17. Solution of the proposed approach integrated with INS during 120 Secs of GNSS signal outage.

As shown in the Figures 17 and 18 that even with 2 min of complete GNSS outage, the proposed approach is still able to bound the drift exhibited by the INS with RMSE in Table 4.

	Proposed approach - INS Error (m)
RMSE North	2.00
Maximum Error North	4.67
RMSE East	2.88
Maximum Error East	6.39

Table 4. Proposed approach performance errors during 120 Secs of GNSS signal outage.

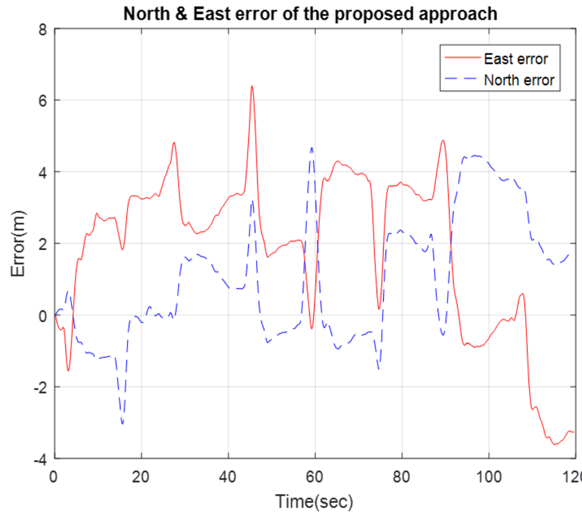

Figure 18. Errors in the north and east direction of the proposed approach INS integration during 120 Secs of GNSS outage.

As shown in the previous 2 experiments that for outage periods reached 2 complete minutes of GNSS signals outage the proposed approach still overcome the INS dead-reckoning solution by more than 99 %.

3.2.5 Proposed approach- INS integration (260 Secs Outage): This last experiment presented in Figure 19 and 20 is to stand on the ability of the proposed approach to still aid the navigation system during longer outage periods (more than 4 minutes of complete absolute positioning system outage).

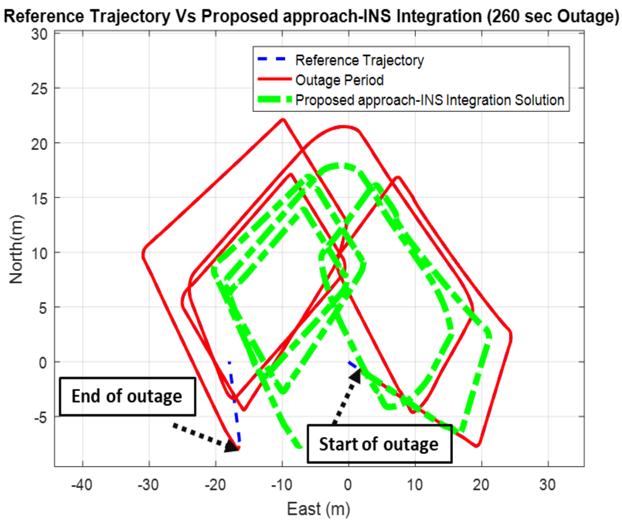

Figure 19. Solution of the proposed approach integrated with INS during 260 Secs of GNSS signal outage

	Proposed approach - INS Error (m)
RMSE North	2.31
Maximum Error North	6.22
RMSE East	4.69
Maximum Error East	10.6

Table 5. Proposed approach performance errors during 260 Secs of GNSS signal outage.

This test showed that for an even longer period of GNSS outage the performance of the proposed approach is still confined within

RMSE 4.69 and 2.31 meters in the east and north direction respectively as shown in Table 5.

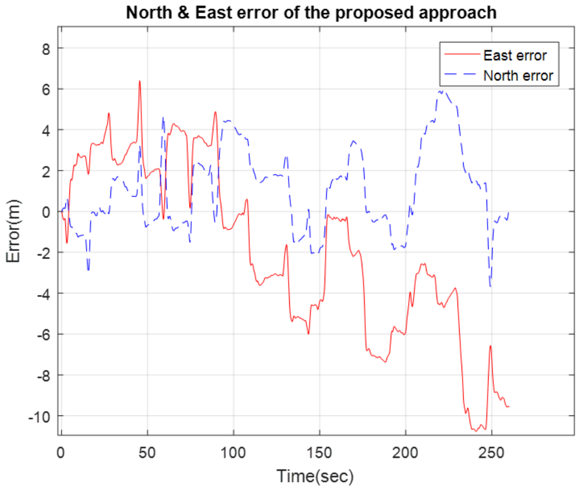

Figure 20. Errors in the north and east direction of the proposed approach integrated with INS during 260 Secs of GNSS signal outage.

To show how this low cost(Air-Odo around 20 CAD, and mass-flow meter around 60 CAD), Lightweight (the overall system weight is less than 85 grams), low power consumption (the overall system power consumption is less than 200 mW) and small size system greatly enhance the performance of the navigation system, some high end INS systems ("IMU-FSAS Inertial Measurement Unit," n.d.), that costs thousands of dollars claims 4.4 RMSE during 60 Secs of GNSS outage, which is still achieved with the proposed approach within 260 Secs GNSS outage.

4. CONCLUSION

Due to the vital rule that the drones play in our current daily lives, it must be versatile to do any task in all circumstances. Small drones mainly depend on integrated GNSS system and low-cost INS system to estimate the navigation parameters. Without GNSS system, low-cost INS exhibit massive drift. Other aiding sensors are utilized to bound the INS drift and enhance the navigation system unknowns' estimation. This paper proposes a combination of two systems that complement each other weaknesses. These systems act as an odometer system for the quadcopter. The first system is Air-Odo which is based on Hall-Effect sensor to measure the forward velocity of the quadcopter. Air-Odo working principle is based on the law of immersed bodies in fluids. The dynamic velocities range of the Air-Odo can be adjusted according to the resisting plate weight. To accommodate for higher velocities the dynamic range of the Air-Odo is changed to cover velocities ranges between 2.5 m/s to 10 m/s. In order to account for the velocities below 2.5m/s other sensor was used (Mass flow sensor). Although Mass-Flow sensor has the ability to measure higher velocities, but its sensitive to the direction of air. Due to quadcopter dynamics way of motion, which requires the quadcopter to tilt more as the velocity increase, Mass-Flow sensor is not useful for quadcopter high tilt motion (higher velocities). Air-Mass flow limitations will be covered by Air-Odo. The proposed system was verified by hardware experiment which includes more than four minutes (260 Secs) of complete GNSS signals outage in indoor field. The results showed a great enhancement in the navigation system reached more than 99% compared to INS as stand alone system.

5. PATENT

Air-Odo is filed on June 6, 2018 in SYSTEM AND METHOD FOR DETERMINING AIRSPEED, U.S. Provisional Application No. 62/681,233.

ACKNOWLEDGEMENTS

This research is under the supervision and funding of Prof. Naser El-Sheimy from NSERC and Canada Research Chairs programs.

6. REFERENCES

Bailey, T., Durrant-Whyte, H., 2006. Simultaneous localization and mapping (SLAM): part II. IEEE Robot. Autom. Mag. 13, 108–117. https://doi.org/10.1109/MRA.2006.1678144

Barton, J.D., 2012. Fundamentals of Small Unmanned Aircraft Flight. Johns Hopkins APL Tech. Dig. 31, 132–149.

Caballero, F., Merino, L., Ferruz, J., Ollero, A., 2009. Unmanned Aerial Vehicle Localization Based on Monocular Vision and Online Mosaicking. J. Intell. Robot. Syst. 55, 323–343. https://doi.org/10.1007/s10846-008-9305-7

Chao, H., Gu, Y., Napolitano, M., 2013. A survey of optical flow techniques for UAV navigation applications, in: 2013 International Conference on Unmanned Aircraft Systems (ICUAS). Presented at the 2013 International Conference on Unmanned Aircraft Systems (ICUAS), pp. 710–716. https://doi.org/10.1109/ICUAS.2013.6564752

Enhanced UAV navigation in GNSS denied environment using repeated dynamics pattern recognition - IEEE Conference Publication [WWW Document], n.d. URL https://ieeexplore-ieee-org.ezproxy.lib.ucalgary.ca/document/8373497 (accessed 9.26.18).

Hemann, G., Singh, S., Kaess, M., 2016. Long-range GPS-denied aerial inertial navigation with LIDAR localization, in: Intelligent Robots and Systems (IROS), 2016 IEEE/RSJ International Conference On. IEEE, pp. 1659–1666.

IMU-FSAS Inertial Measurement Unit [WWW Document], n.d. . Canal Geomat. URL http://www.canalgeomatics.com/product/novatel-imu-fsas-inertial-measurement-unit/ (accessed 12.11.18).

Kumar, G.A., Patil, A.K., Patil, R., Park, S.S., Chai, Y.H., 2017. A LiDAR and IMU Integrated Indoor Navigation System for UAVs and Its Application in Real-Time Pipeline Classification. Sensors 17. https://doi.org/10.3390/s17061268

Lu, Y., Xue, Z., Xia, G.-S., Zhang, L., 2018. A survey on vision-based UAV navigation. Geo-Spat. Inf. Sci. 21, 21–32. https://doi.org/10.1080/10095020.2017.1420509

Mohamed, H.A., Moussa, A.M., Elhabiby, M.M., El-Sheimy, N., Sesay, A.B., 2017. CORNER FEATURES AIDED INDOOR SLAM FOR UNMANNED VEHICLES, in: The 10th International Symposium on Mobile Mapping Technology. Presented at the MMT2017, ISPRS, Cairo, Egypt.

Mostafa, M.M., Moussa, A.M., El-Sheimy, Naser, Sesay, Abu B., "Optical Flow Based Approach for Vision Aided Inertial Navigation Using Regression Trees," *Proceedings of the 2017 International Technical Meeting of The Institute of Navigation*, Monterey, California, January 2017, pp. 856-865. https://doi.org/10.33012/2017.14898

Mustafah, Y.M., Azman, A.W., Akbar, F., 2012. Indoor UAV Positioning Using Stereo Vision Sensor. Procedia Eng., International Symposium on Robotics and Intelligent Sensors 2012 (IRIS 2012) 41, 575–579. https://doi.org/10.1016/j.proeng.2012.07.214

Noureldin, A., Karamat, T.B., Georgy, J., 2013. Fundamentals of Inertial Navigation, Satellite-based Positioning and their Integration. Springer Berlin Heidelberg, Berlin, Heidelberg. https://doi.org/10.1007/978-3-642-30466-8

Sheta, B., 2012. Vision Based Navigation (VBN) of Unmanned Aerial Vehicles (UAV) (Thesis). University of Calgary. http://dx.doi.org/10.11575/PRISM/28646

Tang, J., Chen, Y., Niu, X., Wang, L., Chen, L., Liu, J., Shi, C., Hyyppä, J., 2015. LiDAR Scan Matching Aided Inertial Navigation System in GNSS-Denied Environments. Sensors 15, 16710–16728. https://doi.org/10.3390/s150716710

Valavanis, K.P., Vachtsevanos, G.J., 2015. Future of Unmanned Aviation, in: Valavanis, K.P., Vachtsevanos, G.J. (Eds.), Handbook of Unmanned Aerial Vehicles. Springer Netherlands, Dordrecht, pp. 2993–3009. https://doi.org/10.1007/978-90-481-9707-1_95

Wang, T., Wang, C., Liang, J., Chen, Y., Zhang, Y., 2013. Vision-Aided Inertial Navigation for Small Unmanned Aerial Vehicles in GPS-Denied Environments. Int. J. Adv. Robot. Syst. 10, 276. https://doi.org/10.5772/56660

Zahran, S., Moussa, A., Sesay, A., El-Sheimy, N., 2018a. ENHANCEMENT OF REAL-TIME SCAN MATCHING FOR UAV INDOOR NAVIGATION USING VEHICLE MODEL. ISPRS Ann. Photogramm. Remote Sens. Spat. Inf. Sci. IV–1, 171–178. https://doi.org/10.5194/isprs-annals-IV-1-171-2018

Zahran, S., Moussa, A., Sesay, A.B., El-Sheimy, N., 2018b. A New Velocity Meter based on Hall Effect Sensors for UAV Indoor Navigation. IEEE Sens. J. 1–1. https://doi.org/10.1109/JSEN.2018.2890094

Zhang, C., Chen, J., Song, C., Xu, J., 2014. An UAV navigation aided with computer vision, in: The 26th Chinese Control and Decision Conference (2014 CCDC). Presented at the The 26th Chinese Control and Decision Conference (2014 CCDC), pp. 5297–5301. https://doi.org/10.1109/CCDC.2014.6852209

Zhang, J., Liu, W., Wu, Y., 2011. Novel Technique for Vision-Based UAV Navigation. IEEE Trans. Aerosp. Electron. Syst. 47, 2731–2741. https://doi.org/10.1109/TAES.2011.6034661